Semiconductive and photoconductive properties of the single-molecule magnets Mn_{12}-acetate and Fe_8Br_8

J. M. North, D. Zipse, and N. S. Dalal
Department of Chemistry and Biochemistry, and National High Magnetic Field Laboratory, Florida State University, Tallahassee, Florida 32306-4390

E. S. Choi, E. Jobiliong, J. S. Brooks, and D. L. Eaton
Department of Physics, and National High Magnetic Field Laboratory, Florida State University, Tallahassee, Florida 32306-4390

(Received 18 December 2002; published 13 May 2003)

Resistivity measurements are reported for single crystals of Mn_{12}-acetate and Fe_8Br_8. Both materials exhibit a semiconductor-like, thermally activated behavior over the 200–300 K range. The activation energy E_a obtained for Mn_{12}-acetate was 0.37 ± 0.05 eV, which is to be contrasted with the value of 0.55 eV deduced from the earlier reported absorption edge measurements and the range of 0.3–1 eV from intramolecular density of states calculations, assuming $2E_a = E_g$, the optical band gap. For Fe_8Br_8, E_a was measured as 0.73 ± 0.1 eV, and is discussed in light of the available approximate band structure calculations. Some plausible pathways are indicated based on the crystal structures of both lattices. For Mn_{12}-acetate, we also measured photoconductivity in the visible range; the conductivity increased by a factor of about 8 on increasing the photon energy from 632.8 nm (red) to 488 nm (blue). X-ray irradiation increased the resistivity, but E_a was insensitive to exposure.

DOI: 10.1103/PhysRevB.67.174407 PACS number(s): 75.50.Xx, 72.80.Jc, 72.40.+w

I. INTRODUCTION

The magnetic molecules $[Mn_{12}O_{12}(CH_3COO)_{16}(H_2O)_4] \cdot 2CH_3COOH \cdot 4H_2O$, abbreviated Mn_{12}-ac,[1] and $[(C_6H_{15}N_3)_6Fe_8(\mu_3-O)_2(\mu_2-OH)_{12}]Br_7(H_2O)Br \cdot 8H_2O$, in short Fe_8Br_8,[2] have been the focus of extensive studies since it was discovered that they exhibit the rare phenomenon of macroscopic quantum tunneling (MQT).[3–5] As has now been well established,[3–15] both of these compounds have a net total spin $S = 10$, and can be grown as high quality single crystals.[1,2,6–8] The evidence for MQT consisted of the following observations: (a) below a certain temperature, known as the blocking temperature T_B (2.7 K for Mn_{12}-ac and 1 K for Fe_8Br_8), their magnetic hysteresis loops exhibited sharp steps at regular intervals (about 0.46 T for Mn_{12}-ac and 0.24 T for Fe_8Br_8), when the field was applied along the easy axes[3–6] and (b) the magnetization relaxation rate became temperature independent at low temperatures.[3–6] Furthermore, this quantized hysteretic behavior was found also for very dilute samples, such as frozen into organic solvents.[9] This observation implies that the hysteresis loop is a property of every single molecule, rather than that of a macroscopic domain, hence they have been described as single molecule magnets (SMM's).[10] It can thus be expected that these SMM's hold the potential for becoming an integral part of a molecular-size memory device.[9] Mn_{12}-ac has also been proposed as a potential candidate for a quantum computing element.[11]

To advance our understanding of these materials for possible applications, it is important to understand their electrical conductivity behavior. Although these materials appear to be insulating, they are single crystalline materials with a unique configuration of large molecular units containing transition metal ions and polarizable subunits, nested in a bridging network. One might thus expect some sort of semiconducting behavior, albeit with high resistivity. Interestingly, information about the electrical conductivity is not yet available for either compound, despite the fact that Mn_{12}-ac and Fe_8Br_8 have been studied by dielectric relaxation,[16] far-infrared absorption under applied magnetic fields,[17] Raman scattering,[18–20] micro-Hall techniques,[21,22] micro-SQUID magnetometry,[13,23] EPR,[7,8,24–29] NMR,[30–36] specific heat[37–39] and magnetization measurements,[3–6] neutron scattering,[40–43] and optical absorption.[44] We note, however, that from optical absorption measurements Oppenheimer *et al.*[44] have deduced optical excitation band gaps E_g of 1.1 and 1.75 eV for the minority (inner tetrahedron) and majority (crown) spin systems in Mn_{12}-ac, respectively. These values were considered comparable with corresponding theoretical estimates of 0.45 and 2.08 eV by Pederson and Khanna[45] and of 0.85 and 1.10 eV by Zeng *et al.*[46] In the present investigation we have carried out electrical conductivity measurements on single crystals of both Mn_{12}-ac and Fe_8Br_8 over the temperature range of 77 to 300 K. Confirmatory measurements were made using ac dielectric techniques. The results show that both compounds exhibit fairly clear semiconducting behavior (200–300 K) with distinctly different transport activation energies. It should be noted that in an intrinsic semiconductor, the activation energy (or gap) measured via conductivity is to be compared with $1/2\ E_g$,[47] and thus for Mn_{12}-ac the agreement with the optical data are satisfactory.

We also describe photoconductivity over the visible range and x-ray damage investigations on Mn_{12}-ac to further probe the nature of electrical transport in these materials. The measured photoconductivity exhibits a significant wavelength dependence.

II. EXPERIMENTAL

Long black rectangular crystals of Mn_{12}-ac were synthesized following the procedure of Lis.[1] The crystals typically

grew to dimensions of about $0.5\times0.5\times3.0$ mm^3. High quality single crystals of Fe_8Br_8 were prepared by the method described in the literature.[2] The Fe_8Br_8 crystals grew as dark brown orthorhombic plates of about $4.0\times6.0\times0.5$ mm^3. The samples have been routinely monitored for quality by NMR, x-ray diffraction, and magnetization measurements.

dc resistance measurements were conducted under either a constant voltage or a constant current mode using a conventional four probe technique. A high input impedance (2×10^{14} Ohm) electrometer was used to measure the voltage drop across the sample when constant current was applied. Currents were typically in the 0.1 to 10 nA range, and voltages were generally 100 V or less. The current-voltage characteristics were periodically checked to verify Ohmic behavior. ac conductance measurements were made with a standard ac impedance bridge technique. A capacitive electrode configuration was made by painting two flat parallel surfaces of a sample with conductive (silver or graphite) paste. The capacitive and dissipative signals were detected by a lock-in amplifier with an excitation frequency of about 8 kHz. In all cases the measurements were made under vacuum in a temperature controlled probe.

Photoconductivity measurements were made on Mn_{12}-ac (see Fig. 1) using a He-Ne laser for red (632.8 nm) and argon laser for blue (488 nm) and green (514 nm) light. The light intensity was calibrated before each measurement. Photocurrent was measured using a lock-in amplifier while the sample was under direct current bias and illuminated by chopped light. A more detailed description of the experiment is published elsewhere.[48] For the x-ray experiments, Mn_{12}-Ac crystals were irradiated with 40 kV, 40 mA, Cu K_α radiation at room temperature in order to observe the effects of defects.

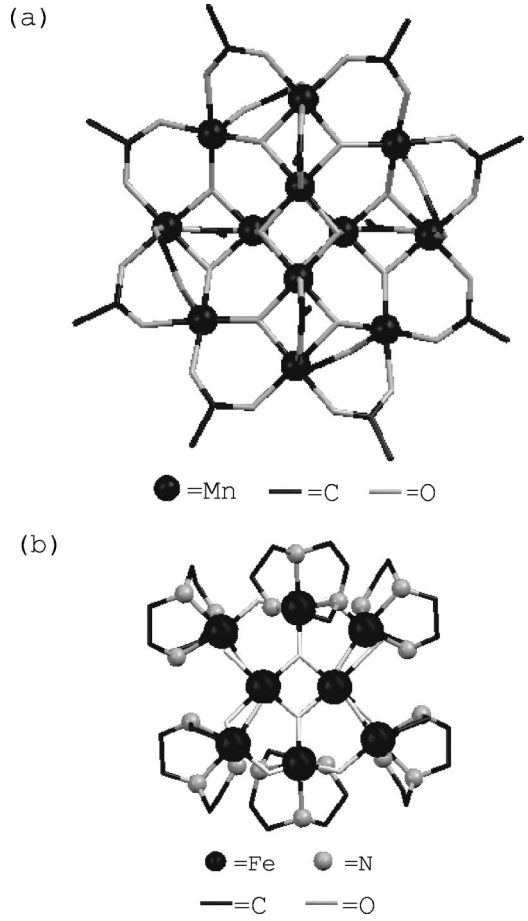

FIG. 1. (a) Structure of Mn_{12}-ac with acetate ligand. The H_2O molecules are omitted for clarity (Ref. 1). (b) Structure of Fe_8Br_8 showing the 1,4,7 triazacyclononane ligand. The Br atoms are omitted for clarity (Ref. 2).

III. RESULTS

A. Conductivity of Mn_{12}-ac

The temperature dependence of the resistance $R(T)$ of a Mn_{12}-ac sample is shown in Fig. 2(a) for a four-terminal, constant current configuration. The resistivity values are on the order of 10^9 Ω cm at room temperature, and increase rapidly in an activated manner upon cooling. Below about 200 K, Ohmic equilibrium is lost due to the high resistance values. Thus the Arrhenius analysis was limited to temperatures above this temperature. Over the 200–300 K range, $\ln R$ exhibits a linear dependence as a function of 1/T as shown in the inset, characteristic of a semiconducting system with a well defined band gap where $R(T)\sim\exp(E_a/k_BT)$, and E_a is the thermal activation energy. From the slopes of curves of the inset, E_a is estimated to be 0.38 ± 0.05 eV.

It seems worthwhile explaining further the plots in Fig. 2(a). The arrows indicate the direction of the temperature change. The sample was first cooled to 77 K with liquid nitrogen. At that temperature the sample became too resistive to measure accurately. The sample was then warmed up by evaporating the coolant, and the resistance measurements were initiated at about 150 K. The saturation of the resistance is an artifact of the experimental setup, and our inability to measure the resistance. With the temperature increase above about 210 K the resistance started to drop, and continued to decline up to 300 K. The cause of the irreversibility in the runs with opposite temperature scans is still not understood. We ascribe it tentatively to the presence of thermally induced defects and/or lattice strain. The two plots are identical from 300 K down to about 240 K. This is the temperature regime where the data were analyzed in terms of an Arrhenius behavior [inset of Fig. 2(a)]. These data were consistent with those obtained with an ac impedance bridge technique as can be noted from Fig. 3.

Figure 2(b) shows the temperature dependence of the current for the constant voltage (50 V) bias condition. As the resistance of the sample increases with decreasing temperature, the current rapidly decreases, and is unmeasurable below ~210 K. The corresponding $\ln R$ vs $1/T$ curve is shown in the inset. The linear dependence yields a value of $E_a=0.36\pm0.05$ eV.

Figure 3 shows the $\ln R$ vs $1/T$ curve of a Mn_{12}-ac sample obtained by the impedance bridge technique. The sample

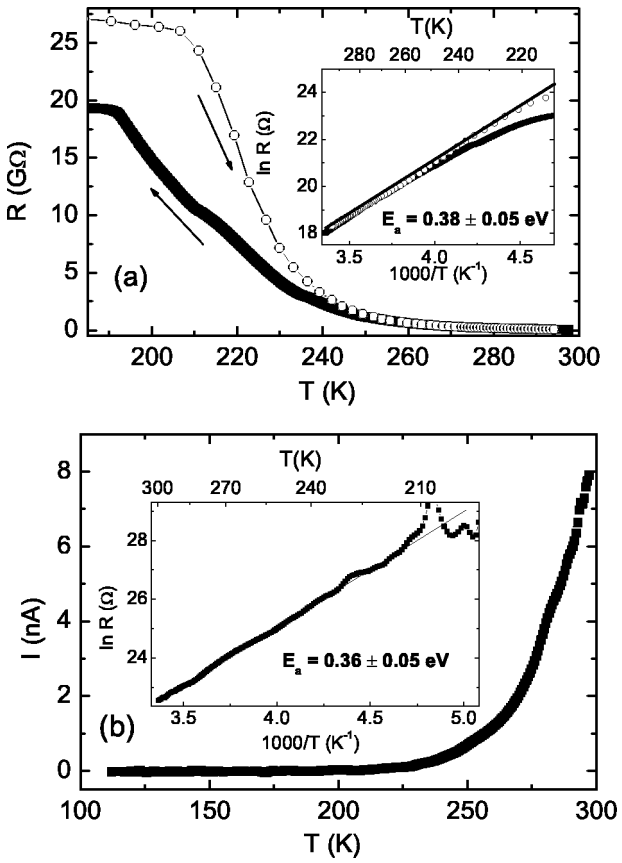

FIG. 2. (a) Temperature dependence of resistance $R(T)$ of Mn_{12}-ac measured at a constant dc condition. The arrows indicate cooling and warming curves. Inset: $\ln R$ vs $1/T$ curve yields $E_a = 0.38 \pm 0.05$ eV. (b) Temperature dependence of measured current under a constant voltage bias (50 V). Inset: $\ln R$ vs $1/T$ curve where $E_a = 0.36 \pm 0.05$ eV.

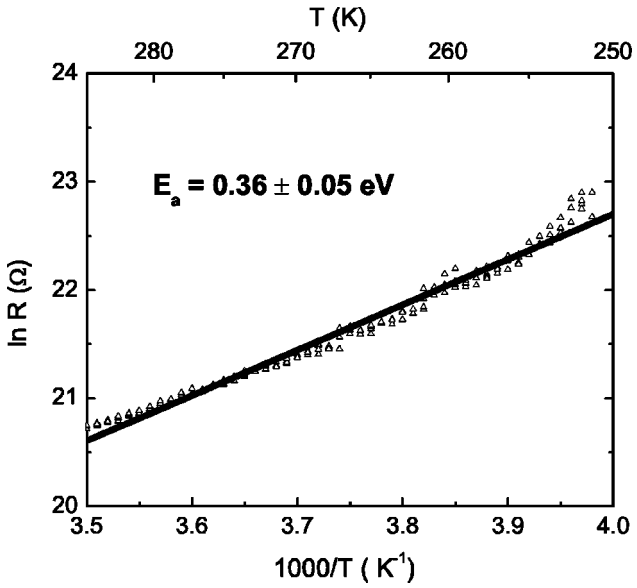

FIG. 3. $\ln R(T)$ vs $1/T$ curve of Mn_{12}-ac measured with the ac impedance bridge technique. The sample was cooled from room temperature to 200 K. The solid line is for the curve resulting in $E_a = 0.36 \pm 0.05$ eV.

was cooled from room temperature to 200 K. The solid line corresponds to $E_a = 0.36 \pm 0.05$ eV. The resistance again shows activated behavior but the linear relation is not so clear as in the dc resistance case.

A significant observation was that the Mn_{12}-ac crystals lose solvent upon heating above 300 K. One sample was heated to 350 K and then cooled down to 200 K. The plot of $\ln R$ vs $1/T$ yielded two separate straight lines as can be noted from Fig. 4. The measured activation energy at the higher temperature range was 0.35 ± 0.05 eV, while it was 0.18 ± 0.05 eV for the lower temperatures, after heating. Thus, care must be taken not to heat the samples above 300 K or so.

B. Photoconductivity of Mn_{12}-ac

Photoconductivity (PC) was measured on Mn_{12}-ac using the ac component of the photocurrent for chopped laser light illumination. This was done by biasing the sample with different values of dc current.[48] Figure 5 shows the dependence of the PC on the intensity (power) of the laser radiation at the three wavelengths used, 632.8 nm (red), 514 nm (green), and 488 nm (blue). PC is seen to increase with photon energy. The increase is about a factor of 8 when going from 632.8 to 488 nm. Clearly this enhancement must relate to the creation of charge carriers by the photons, or to the increase in temperature due to light absorption, or both. A simple thermal mechanism is not supported by the earlier UV-visible absorption data of Oppenheimer *et al.*[44] on Mn_{12}-ac. The spectra show a gradual increase in absorption with photon energy and the absorption edge was estimated to be about 1.1 eV. However, over the 632.8 to 488 nm range, the absorption was nearly (within a factor of 2) constant,

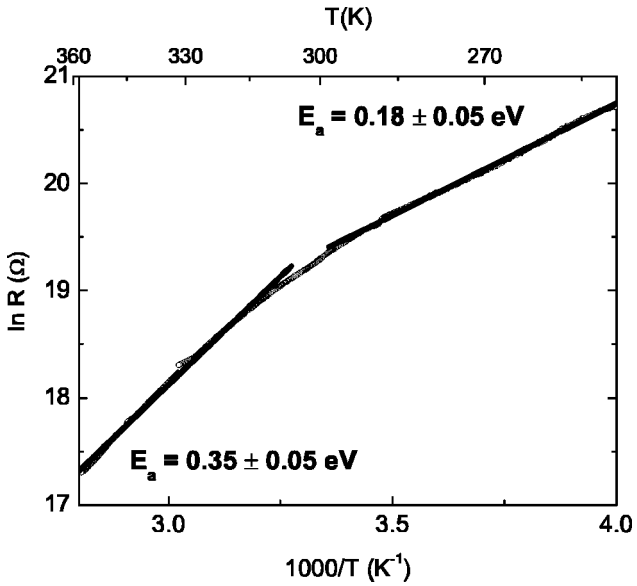

FIG. 4. Mn_{12}-ac sample which was heated to 350 K and then cooled down to 200 K. Straight lines show an $E_a = 0.35 \pm 0.05$ eV for the high temperature region, and 0.18 ± 0.05 eV for the low temperature region.

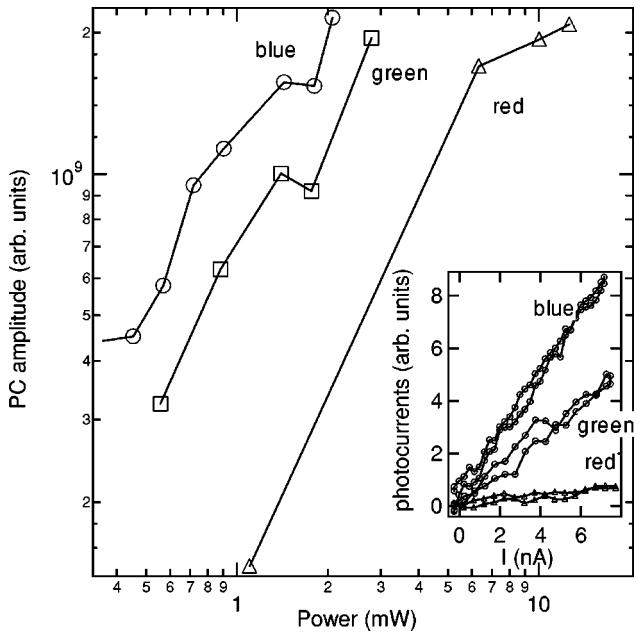

FIG. 5. Photoconductivity signal of Mn_{12}-ac as a function light intensity induced by different wavelengths of light (red: 632.8 nm, green: 514 nm, and blue: 488 nm). The inset shows the ac photocurrent as a function of applied dc current when the light intensity is about 1 mW. Data for both increasing and decreasing direct current bias are shown.

while the PC increases by a factor of 8. These considerations argue against a major role of thermal heating in the mechanism of the observed PC enhancement. The effect is thus ascribed to an enhancement of charge carriers due to optical absorption.

C. Effect of x-ray irradiation on Mn_{12}-ac

Recently, Hernandez *et al.*[49] observed an increase in the magnetization tunneling rate of Mn_{12}-ac caused by defects in the lattice as a result of x-ray irradiation and heat treatments. In order to probe the possible role of defects in the transport properties of Mn_{12}-ac, we have also carried out an x-ray irradiation study. As the irradiation dose was increased from 2 to 20 h, the overall resistivity of the sample increased, but a plot of $\ln R$ vs $1/T$ for the different exposure times showed the activation energies remained fairly constant. The radiation-induced defects thus seem to act as trapping sites for the carriers. This effect is further discussed in Sec. IV.

D. Conductivity of Fe_8Br_8

Preliminary temperature dependent conductivity measurements have also been carried out on single crystals of Fe_8Br_8. Figure 6 shows a typical $\ln R(T)$ vs $1/T$ plot. The slope of the line yields a value of $E_a = 0.73 \pm 0.1$ eV, which is seen to be significantly higher than that of Mn_{12}-ac (0.37 ± 0.05 eV). This is discussed later in terms of the bonding of Fe_8Br_8 and Mn_{12}-ac. At present no optical data are available for Fe_8Br_8 for comparison with the conductivity measurements. Table I summarizes the conductivity results in comparison to the optical data[44] and theoretical calculations.[45,46,50]

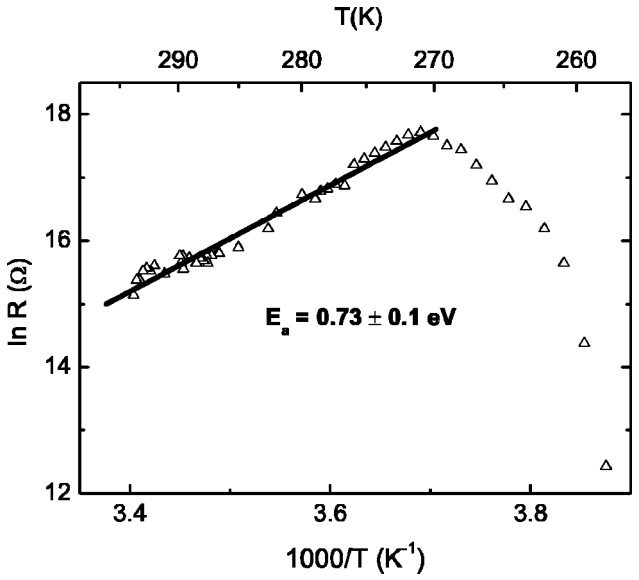

FIG. 6. Plot of $\ln R(T)$ vs $1/T$ for Fe_8Br_8. The solid line yields a value of $E_a \approx 0.73 \pm 0.1$ eV.

IV. DISCUSSION

The main result of this study of the electrical transport in these SMM-type single crystalline materials is that they exhibit thermally activated conductivity characteristic of a gapped semiconductor over the range of 200–300 K. Photoconductivity measurements also support their description as gapped semiconductors. However, the precise nature of the carrier transport is difficult to determine, since generally measurements over many orders of magnitude in temperature are necessary to establish the functional dependence of

TABLE I. Comparison of E_g from conductivity and optical data, and theoretical calculations.

	Conductivity	Optical	Theoretical
Mn_{12}-ac	0.74 ± 0.1 eV [a]	1.08 eV [b]	0.45 eV [c]
		1.75 eV [d]	2.08 eV [e]
			0.85 eV [f]
			1.10 eV [g]
Fe_8Br_8	1.46 ± 0.2 eV [a]		0.9 eV [h]
			0.9 eV [i]

[a]Present work, assuming $E_g = 2E_a$.
[b]Oppenheimer *et al.* (Ref. 44), minority spin cluster.
[c]Pederson *et al.* (Ref. 45), minority spin cluster.
[d]Oppenheimer *et al.* (Ref. 44), majority spin cluster.
[e]Pederson *et al.* (Ref. 45), majority spin cluster.
[f]Zeng *et al.* (Ref. 46), minority spin cluster.
[g]Zeng *et al.* (Ref. 46), majority spin cluster.
[h]Pederson *et al.* (Ref. 50), minority spin cluster.
[i]Pederson *et al.* (Ref. 50), majority spin cluster.

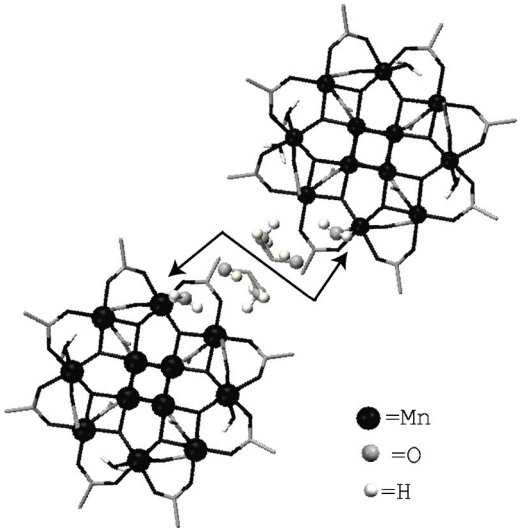

FIG. 7. Schematic of proposed conduction path between two Mn_{12}-ac molecules.

$R(T)$. In order to understand the conduction pathway, we examined the connectivity between the neighboring Mn_{12}-ac and Fe_8Br_8 clusters. Figures 7 and 8 show several transport scenarios are possible. First, as a result of the crystalline lattice, one can expect that there will be a band structure with gaps. At present, only the electronic structure of the clusters has been computed.[45,46] For a band-gapped semiconductor, one expects the resistivity to vary as $\exp(E_a/k_BT)$, where E_a is related to the optical gap E_g by $E_g=2E_a$.[47] However, due to the complexity of the crystal structure, it is possible that impurities and/or disorder play significant roles in the charge transport. For example, thermally activated hopping between impurity sites can also give similar temperature dependence.

If conduction is through a distribution of impurity sites, variable range hopping (VRH) should dominate. However, the following considerations argue against a VRH behavior. Furthermore, the resistivity ($\sim 10^9$ Ω cm) is very high for a typical VRH conduction system.[51] Moreover, application of the Mott formula for VHR [$R(T)\sim\exp(T_0/T)^{\gamma}$, with $\gamma=1/(1+d)$, where d is the dimensionality] yielded $T_0\approx 3\times 10^9$ K (for $d=3$). The high sensitivity of the VRH model to defects can be tested by introducing them artificially, by ion implantation, or in the present case, by x-ray irradiation. Since the T_0 values obtained from the Mott formula indicate an extremely small density of impurity sites, i.e., $N(E_F)$, a small number of additional defects should decrease T_0 significantly. However, our experimental results on irradiated samples (Sec. III C) indicate that T_0 and E_a are insensitive to the creation of defects. Hence the x-ray investigation supports the idea of intrinsic semiconductor-like conduction in Mn_{12}-ac, and by inference, also for Fe_8Br_8.

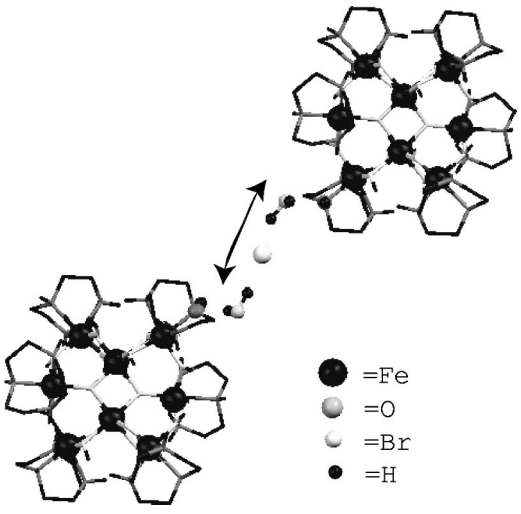

FIG. 8. Conduction pathway between two Fe_8Br_8 molecules.

While we have not been able to arrive at any detailed picture of the conduction pathways, we offer the following possibilities based on the structure and bonding characteristics of both lattices. The pathway for Mn_{12}-ac is based upon simple Coulombic interactions between Mn^{3+} ions, and the polar molecules which lie between two Mn_{12}-ac clusters. A water molecule bound to a Mn^{3+} on the outer crown lies 2.67 Å away from an unbound acetate ligand, which is, in turn, 2.77 Å away from a symmetrically equivalent, unbound acetate ligand adjacent to the closest Mn_{12}-ac cluster as seen in Fig. 7. The Fe_8Br_8 conduction pathway is illustrated in Fig. 8. The proposed pathway between two Fe_8Br_8 clusters is through an N-H bond in the 1,4,7-triazacyclononane. The conduction pathway thus extends from the N-H to a water (2.4 Å), to a Br^- (2.3 Å), to a water (2.1 Å), and finally to a hydrogen (2.4 Å) directly connected to the 1,4,7-triazacyclononane on the adjacent Fe_8Br_8. It should be noted that the proposed Mn_{12}-ac conduction pathway is much more direct than that for Fe_8Br_8. This is consistent with the higher activation energy found for Fe_8Br_8.

V. SUMMARY

We have found that both Mn_{12}-ac and Fe_8Br_8 exhibit a gapped semiconductor-like behavior in their electrical transport properties. The limited temperature range over which the resistance was measurable, and over which the materials are stable, restricts a knowledge of the precise functional form of $R(T)$. Nevertheless, complementary photoconductivity and x-ray irradiation studies support a model where the transport is governed by a well-defined energy gap. The E_a's have been determined to be 0.37 ± 0.05 and 0.73 ± 0.1 eV for Mn_{12}-ac and Fe_8Br_8, respectively. Assuming an intrinsic semiconducting behavior, they lead to E_g values of 0.74 ± 0.10 eV for Mn_{12}-ac and 1.5 ± 0.2 eV for Fe_8Br_8. For Mn_{12}-ac, the agreement is seen to be reasonably good with the optical band gaps for minority (inner tetrahedron) spins, and the theoretical estimates by Pederson and Khanna[45] as well as Zeng *et al.*[46] (see also Katsnelson *et al.*[52]). Additional optical and theoretical data are needed for Fe_8Br_8. At present, calculations exist only for the molecular band gaps, but not for the entire lattice. Hence, we can only speculate that the intercluster ligand bridges may play an important role in the conduction mechanism. Further computations on the full crystal band structure are thus desirable.

ACKNOWLEDGMENT

We would like to thank Dr. X. Wei for his assistance in the optical measurements. This work was supported by NSF-DMR Grant No. 023532, DARPA, and NSF/NIRT-DMR Grant No. 0103290. The National High Magnetic Field Laboratory is supported through a cooperative agreement between the National Science Foundation and the State of Florida.

[1] T. Lis, Acta Crystallogr., Sect. B: Struct. Crystallogr. Cryst. Chem. **36**, 2042 (1980).
[2] K. Weighardt, K. Pohl, I. Jibril, and G. Huttner, Angew. Chem., Int. Ed. Engl. **23**, 77 (1984).
[3] J.R. Friedman, M.P. Sarachik, J. Tejada, and R. Ziolo, Phys. Rev. Lett. **76**, 3830 (1996).
[4] L. Thomas, F. Lionti, R. Ballou, D. Gatteschi, R. Sessoli, and B. Barbara, Nature (London) **383**, 145 (1996).
[5] C. Sangregorio, T. Ohm, C. Paulsen, R. Sessoli, and D. Gatteschi, Phys. Rev. Lett. **78**, 4645 (1997).
[6] J.A.A.J. Perenboom, J.S. Brooks, S. Hill, T. Hathaway, and N.S. Dalal, Phys. Rev. B **58**, 330 (1998).
[7] S. Hill, J.A.A.J. Perenboom, N.S. Dalal, T. Hathaway, T. Stalcup, and J.S. Brooks, Phys. Rev. Lett. **80**, 2453 (1998).
[8] S. Hill, S. Maccagnano, K. Park, R.M. Achey, J.M. North, and N.S. Dalal, Phys. Rev. B **65**, 224410 (2002).
[9] E.M. Chudnovsky and J. Tejada, *Macroscopic Quantum Tunneling of the Magnetic Moment* (Cambridge University Press, Cambridge, 1998).
[10] S.M.J. Aubin, M.W. Wemple, D.M. Adams, H. Tsai, G. Christou, and D.N. Hendrickson, J. Am. Chem. Soc. **118**, 7746 (1996).
[11] M.N. Leuenberger and D. Loss, Nature (London) **410**, 789 (2001).
[12] E.M. Chudnovsky and D.A. Garanin, Phys. Rev. Lett. **87**, 187203 (2001); Phys. Rev. B **65**, 094423 (2002).
[13] W. Wernsdorfer, T. Ohm, C. Sangregorio, R. Sessoli, D. Mailly, and C. Paulsen, Phys. Rev. Lett. **82**, 3903 (1999).
[14] F. Luis, J. Bartolome, J.F. Fernandez, J. Tejada, J.M. Hernandez, X.X. Zhang, and R. Ziolo, Phys. Rev. B **55**, 11 448 (1997).
[15] J.F. Fernandez, F. Luis, and J. Bartolome, Phys. Rev. Lett. **80**, 5659 (1998).
[16] Z. Kutnjak, C. Filipic, A. Levstik, R.M. Achey, and N.S. Dalal, Phys. Rev. B **59**, 11 147 (1999).
[17] A.B. Sushkov, B.R. Jones, J.L. Musfeldt, Y.J. Wang, R.M. Achey, and N.S. Dalal, Phys. Rev. B **63**, 214408 (2001); A.B. Sushkov, J.L. Musfeldt, Y.J. Wang, R.M. Achey, and N.S. Dalal, *ibid.* **66**, 144430 (2002).
[18] J.M. North, L.J. van de Burgt, and N.S. Dalal, Solid State Commun. **123**, 75 (2002).
[19] J.M. North, R.M. Achey, and N.S. Dalal, Phys. Rev. B **66**, 174437 (2002).
[20] J. M. North and N. S. Dalal, J. Appl. Phys. (to be published).
[21] L. Bokacheva, A.D. Kent, and M.A. Walters, Phys. Rev. Lett. **85**, 4803 (2000).
[22] K.M. Mertes, Y. Suzuki, M.P. Sarachik, Y. Paltiel, H. Shtrikman, E. Zeldov, E.M. Rumberger, D.N. Hendrickson, and G. Christou, Phys. Rev. B **65**, 212401 (2002).
[23] W. Wernsdofer, R. Sessoli, and D. Gattteschi, Europhys. Lett. **47**, 254 (1999).
[24] A. Mukhin, V.D. Travkin, A.K. Zvezdin, S.P. Lebedev, A. Caneschi, and D. Gatteschi, Europhys. Lett. **44**, 778 (1998).
[25] A. Mukhin, B. Gorshunov, M. Dressel, C. Sangregorio, and D. Gatteschi, Phys. Rev. B **63**, 214411 (2001).
[26] M. Dressel, B. Gorshunov, K. Rajagopal, S. Vongtragool, and A.A. Mukhin, Phys. Rev. B **67**, 060405 (2003).
[27] A.L. Barra, D. Gatteschi, and R. Sessoli, Phys. Rev. B **56**, 8192 (1997).
[28] R. Blinc, P. Cevc, D. Arcon, N.S. Dalal, and R.M. Achey, Phys. Rev. B **63**, 212401 (2001).
[29] K. Park, M.A. Novotny, N.S. Dalal, S. Hill, and P.A. Rikvold, Phys. Rev. B **65**, 014426 (2001); J. Appl. Phys. **91**, 7167 (2002).
[30] A. Lascialfari, Z.H. Jang, F. Borsa, P. Carretta, and D. Gatteschi, Phys. Rev. Lett. **81**, 3773 (1998).
[31] Y. Furukawa, K. Watanabe, K. Kumagai, Z.H. Jang, A. Lascialfari, F. Borsa, and D. Gatteschi, Phys. Rev. B **62**, 14 246 (2000).
[32] D. Arcon, J. Dolinsek, T. Apih, R. Blinc, N.S. Dalal, and R.M. Achey, Phys. Rev. B **58**, 2941 (1998); J. Dolinsek, D. Arcon, R. Blinc, P. Vonlanthen, H.R. Ott, R.M. Achey, and N.S. Dalal, Europhys. Lett. **42**, 691 (1998).
[33] R.M. Achey, P. Kuhns, A. Reyes, W. Moulton, and N.S. Dalal, Polyhedron **20**, 1745 (2001); Phys. Rev. B **64**, 064420 (2001); Solid State Commun. **121**, 107 (2002).
[34] T. Goto, T. Kudo, T. Koshida, Y. Fujii, A. Oyamada, J. Arai, K. Takeda, and K. Awaga, Physica B **284-288**, 1227 (2000).
[35] Y. Furukawa, K. Watanabe, K. Kumagai, F. Borsa, and D. Gatteschi, Phys. Rev. B **64**, 104401 (2001).
[36] T. Kubo, T. Goto, T. Koshiba, K. Takeda, and K. Awaga, Phys. Rev. B **65**, 224425 (2002).
[37] A.M. Gomes, M.A. Novak, R. Sessoli, A. Caneschi, and D. Gatteschi, Phys. Rev. B **57**, 5021 (1998).
[38] F. Fominaya, J. Villain, P. Gandit, J. Chaussy, and A. Caneschi, Phys. Rev. Lett. **79**, 1126 (1997).
[39] M. Sales, J.M. Hernandez, J. Tejada, and J.L. Martinez, Phys. Rev. B **60**, 14 557 (1999).
[40] S. Carretta, E. Liviotti, G. Amoretti, R. Caciuffo, A. Caneschi, and D. Gatteschi, Phys. Rev. B **65**, 052411 (2002).
[41] M. Hennion, L. Pardi, I. Mirebeau, E. Suard, R. Sessoli, and A. Caneschi, Phys. Rev. B **56**, 8819 (1997).
[42] I. Mirebeau, M. Hennion, H. Casalta, H. Andres, H.U. Gudel, A.V. Irodova, and A. Caneschi, Phys. Rev. Lett. **83**, 628 (1999).
[43] R. Caciuffo, G. Amoretti, A. Murani, R. Sessoli, A. Caneschi, and D. Gatteschi, Phys. Rev. Lett. **81**, 4744 (1998).
[44] S.M. Oppenheimer, A.B. Sushkov, J.L. Musfeldt, R.M. Achey, and N.S. Dalal, Phys. Rev. B **65**, 054419 (2002).
[45] M.R. Pederson and S.N. Khanna, Phys. Rev. B **60**, 9566 (1999).
[46] Z. Zeng, D. Guenzburger, and D.E. Ellis, Phys. Rev. B **59**, 6927 (1999).
[47] C. Kittel, *Introduction to Solid State Physics*, 7th ed. (Wiley, New York, 1986), Chap. 8.
[48] T. Tokumoto, J.S. Brooks, R. Clinite, X. Wei, J.E. Anthony, D.L.

Eaton, and S.R. Parkin, J. Appl. Phys. **92**, 5208 (2002).
[49] J.M. Hernandez, F. Torres, J. Tejada, and E. Molins, cond-mat/0110515 (unpublished).
[50] M.R. Pederson, J. Kortus, and S.N. Khanna, J. Appl. Phys. **91**, 7149 (2002).
[51] N.F. Mott and E.A. Davis, *Electronic Processes in Non-Crystalline Materials*, 2nd ed. (Oxford University Press, London, 1979).
[52] M. I. Katsnelson, V. V. Dobrovitski, and B. N. Harmon, Phys. Rev. B **59**, 6919 (1999).